2734

HIGH-RESOLUTION STEREO TOPOGRAPHY RE-EXAMINATION OF CENTRAL ARTEMIS, VENUS

Daniel C. Nunes[1], S. E. Smrekar[1], Nils Muller[2], Joann Stock[3], Anne Davaille[4], Scott Hensley[1], Kevin Cotton[1], and Karl Mitchell[1]

[1]Jet Propulsion Laboratory, California Institute of Technology; [2]German Aerospace Center (DLR), Institute of Planetary Research; [3]California Institute of Technology; [4]Laboratoire FAST, CNRS, Univ. Paris-Sud, Université Paris-Saclay

Daniel.Nunes@jpl.nasa.gov

LPSC 51 LUNAR AND PLANETARY SCIENCE CONFERENCE
THE WOODLANDS, TX MARCH 16–20, 2020

First identified in Pioneer Venus radar altimetry data [1], Artemis chasma hosts extensive contractional and extensional tectonic signatures and volcanic flows in its interior domain, suggesting abundant tectonic and volcanic activity in its history. Despite it being classified as a corona based on its volcanotectonic nature and circular aspect as revealed by Magellan synthetic aperture (SAR) data [2], its gigantism before all other coronae led to a common belief that, if not a unique corona, Artemis may be a feature in a class of its own. Previous analyses of its tectonic and flexural signatures state that Artemis suffered contractional folding then extensional rifting of its interior before overthrusting the neighboring lithosphere to the southeast [3, 4]. Further, significant tracts of the areas surrounding Artemis contain multiple tectonic elements with orientations geometrically correlated with the shape and position of Artemis itself. A favored interpretation of these observations is that Artemis is the surface expression of a major mantle upwelling that dominated the geodynamic history of Venus between an early thin-lid regime and a late fracture-zone tectonism [6, 7]. Tectonic features at the central portion of Artemis surrounding Britomartis Chasma have some signatures resembling complexes that occur under spreading regimes [5], not inconsistent with the interpretation of Artemis as a major mantle upwelling.

Here we present a new look at the central portion of Artemis with a newly-derived, soon to be PDS-archived digital elevation model (DEM) data set that derives from both cross-cycle (Cycle-1/Cycle-3) and intra-cycle (Cycle-1/Cycle-1, Cycle-2/Cycle-2, and Cycle-3/Cycle-3) coverage of the synthetic aperture radar (SAR) images. Specifically, we investigate the topography of the central Britomartis ridge/trough feature and compare it to simple geodynamic models and some terrestrial ocean-floor features.

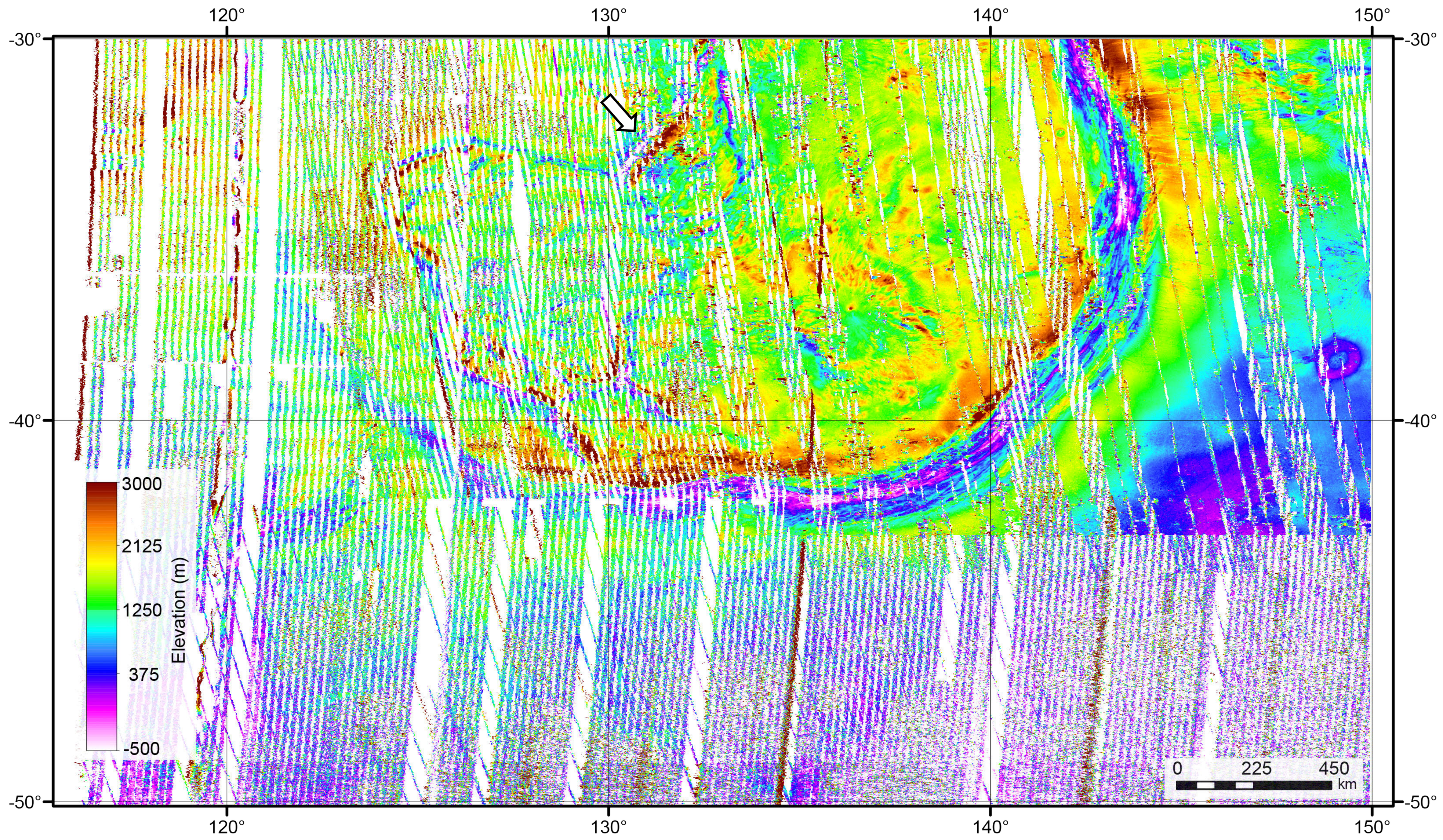

Magellan Stereo DEM of Artemis using Cycles 1/1, 2/2 and 1/3. Britomartis Chasma is denoted by arrow, and shown below

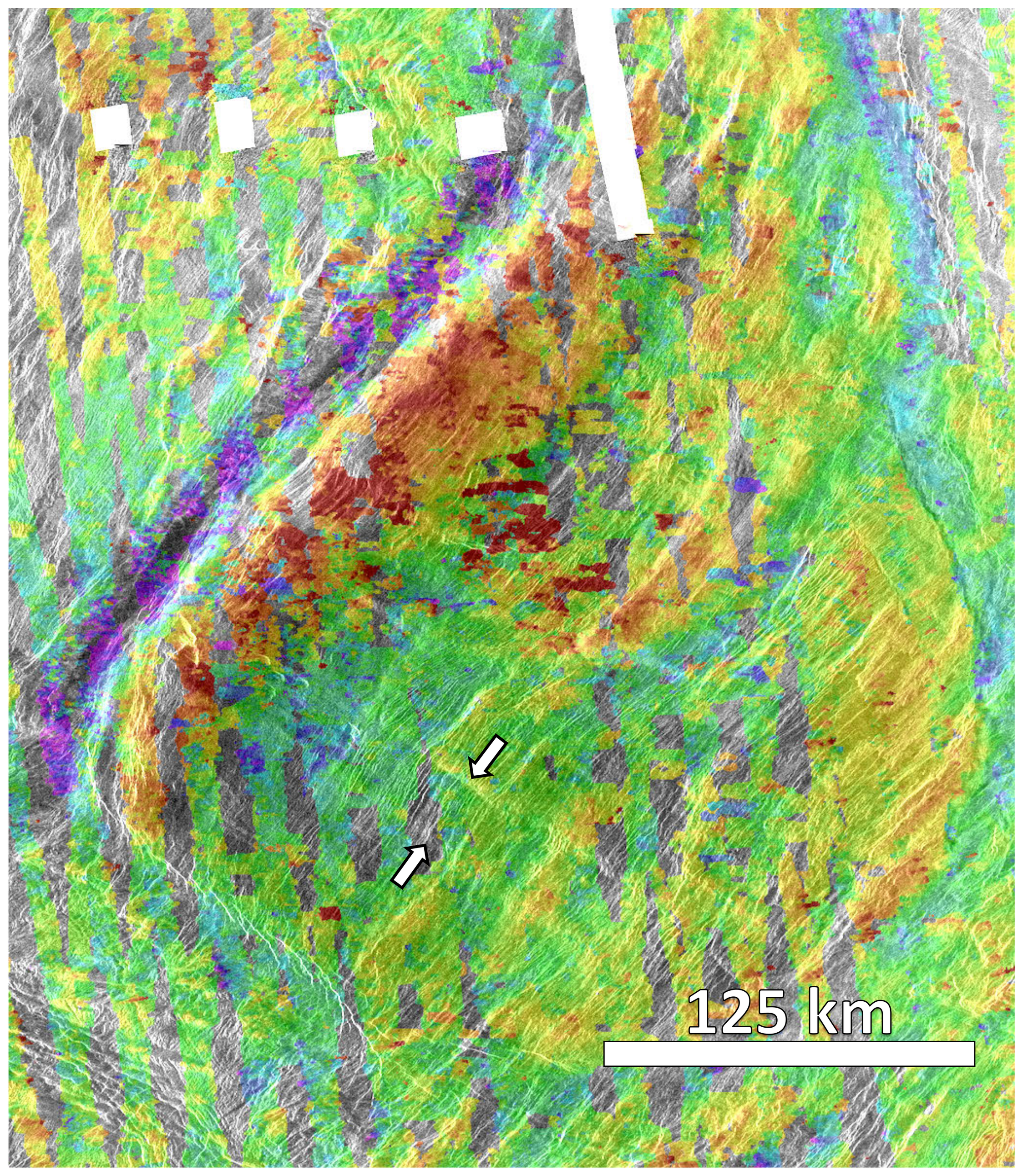

Close up view of stereo DEM over Britomartis Chasma in central Artemis. Highest portions of the ridge lie at elevations between 3500 and 4000 m. Immediately to the NW and parallel to the ridge is a deep trough, the deepest portions of which lie at -2000 m. Arrows denote the lateral boundaries of groove similar to those found in oceanic core complexes.

Reddish blocky area in the middle of the image corresponds to matching blunders; stereo DEM has not been bundle adjusted and corresponds to the raw output of our processing pipeline.

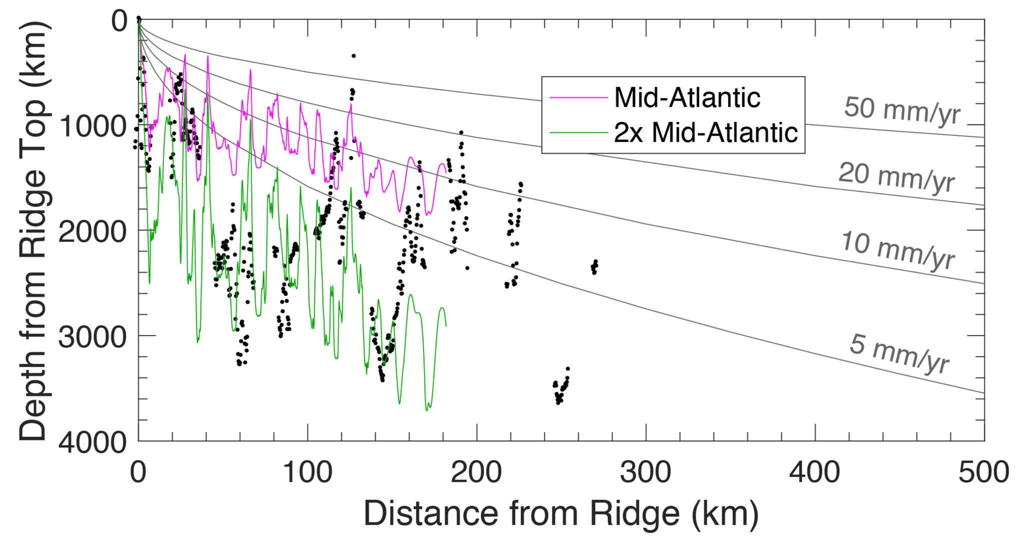

Cross-strike profile (dots), from the top of Britomartis ridge to the SE, compared to halfspace cooling models at different spreading rates. Also Included for reference is a profile (magenta) across the North Atlantic mid-ocean ridge seen on the left; the same profile is shown with 2X exaggerated relief.

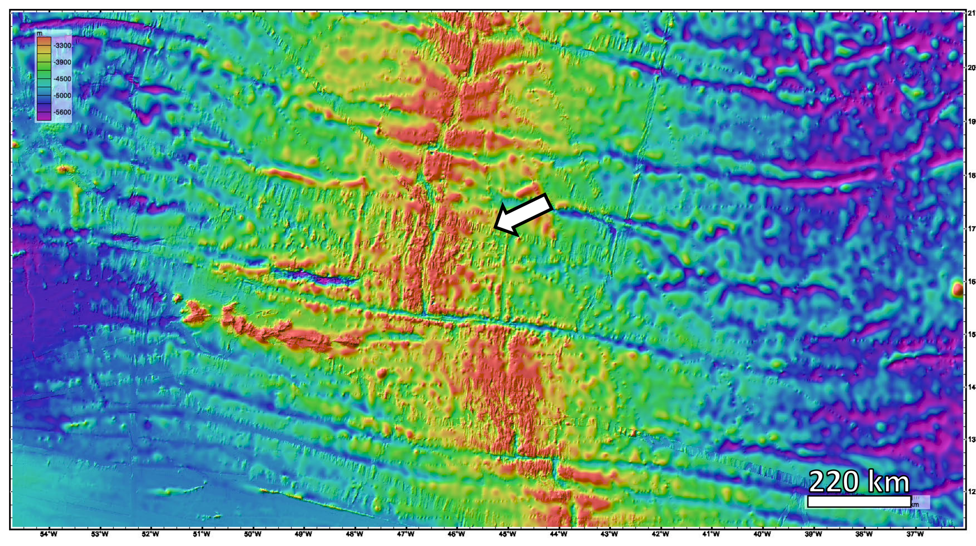

North Atlantic slow spreading mid-ocean ridge bathymetric data, showing 2900 of vertical relief. Scale of this figure is the same as in the Artemis map above. Arrow denotes location of core complex shown below.

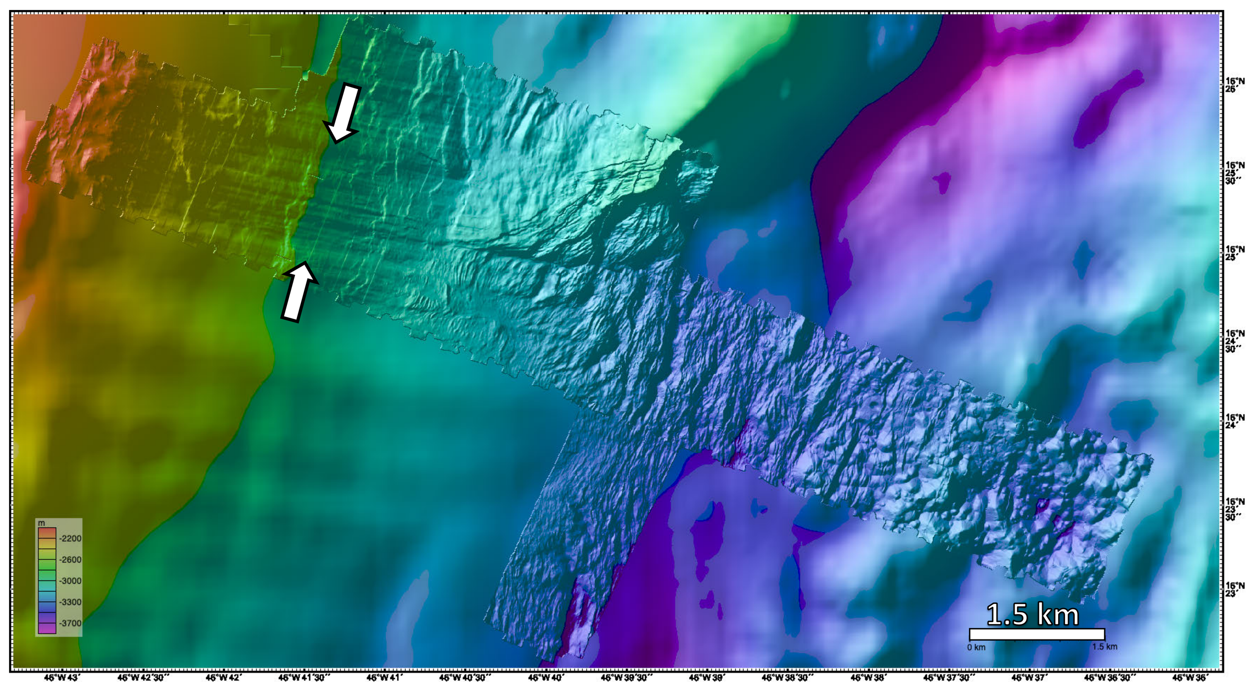

High-resolution bathymetric data at a core complex found in the mid ocean depicted in the above figure, showing 1900 of vertical relief.

Arrows denote lateral boundaries of groove along the direction of spreading

The hypothesis of a core complex for central Artemis offered by [5] is based on the subtle linear features that extend away and at a high-angle from the Britomartis ridge, as seen in the SAR images and interpreted as grooves. Although subtle in SAR, we believe there is topographic evidence for these grooves as well, especially when looking at the highest stereo resolution data, afforded by the cross-cycle data. Unfortunately, it is at this location where Cycle-3 is noisy and broken, so only a few patches of highest resolution are available. Still, where measurable, the grooves display a relief of a few hundred meters. A VIRTIS anomaly over central Artemis was initially detected [18] based on the GTDR. We are currently assessing this anomaly but have found that the narrowing of the ridge/trough feature due to higher resolution of the stereo DEM makes both the topographic correction and emissivity anomaly less significant.

Analysis of our stereo topography is ongoing for Britomartis and the interior deformation in Artemis. At its central portion, the new DEM reveals multiple ridges and troughs associated with the topographic subsidence to the southeast and away from Britomartis. These are subtle to discern in SAR and are similar to faulted blocks in terrestrial spreading centers, albeit larger in amplitude than the specific reference case we used. Groves previously leading to the hypothesis of a core complex are visible in the new DEM. Our findings thus far support an interpretation of a spreading center.

References: [1] Masursky H. et al. (1980) JGR 85, 8232-8260. [2] Stofan E.R. et al. (1992) JGR 97, 13347-13378. [3] Brown C.D. and R.E. Grimm (1995) Icarus 117, 219-249. [4] Brown C.D. and R.E. Grimm (1996) JGR 101, 12697-12708. [5] Spencer J.E. (2001) GSA Bull. 113, 333-345. [6] Hansen V.L. and I. López (2018) JGR 123, 1760-1790. [7] Hansen V.L. and A. Olive (2010) Geology 38, 467-470. [8] Smrekar S.E. et al. (2010) Science 328, 605-608. [9] Herrick R.R. et al. (2012) Eos 93, 125-126. [10] Howington-Kraus E. et al. (2006) EPSC, 490. [11] Hensley S. and S. Shaffer (1994) IGARSS, 1470-1472. [12] Nunes D.C. et al. (2013) AGU Fall Meet., P41D-1961. [13] Hensley S. et al (2016) EUSAR, 1-4. [14] Hensley, S. et al. (2019) IGARSS, 6023-6026. [15] Macdonald K.C. et al. (1996) Nature 380, 125-129. [16] Sibrant A.L.R. et al. (2018) Nature Geosci. 11, 274-279. [17] Whitney D.L. et al. (2013) GSA Bull. 125, 273-298. [18] Mueller N. et al. (2008) JGR 113, E00B18.